UDC: 621.315.592

MICROSCOPY AND MOSSBAUER STUDIES OF IRON STATES IN DOPED GALLIUM ANTIMONIDE

Turtă C.[1], Teodorescu V.[2], Mihălache A.[3*], Gheorghiţă E.[3], Volodina G.[4], Filoti G.[2]

[1]Institute of Chemistry, Academy of Sciences of Moldova, MD 2028 Chisinău, Academiei str. 3, Republic of Moldova

[2]National Institute of Materials Physics, Atomistilor str. 105 bis, P.O.Box MG-7, Ro-077125, Bucharest, Măgurele, Romania

[3]Tiraspol State University, Moldova, MD 2069 Chisinău, Gh. Iablocichin str. 5, Republic of Moldova

[4]Institute of Applied Physics, Academy of Sciences of Moldova, MD 2028 Chişinău, Academiei str. 5, Republic of Moldova

[*]e-mail: alexei.mihalache@gmail.com

A single crystal of gallium antimonide doped with 3 at.% ^{57}Fe was obtained via the Czochralski method. The Mössbauer investigations revealed four iron patterns - one diamagnetic and three Fe magnetically ordered sites, even at room temperature. The data suggested that iron containing compounds are formed at grain boundaries and the microscopy images revealed the presence of two types of boundaries and holes of different shape and size. The EDX spectrum provided different amounts of Fe in the crystal (GaSb) and, respectively, at the boundary area.

Keywords: gallium antimonide, iron-57, Mössbauer spectra, microscopy investigation

Monocristale omogene de antimonidul de galiu dopat cu izotopul de ^{57}Fe au fost crescute prin metoda zonei topite. Măsurătorile spectrelor Mössbauer la temperatura camerei demonstrează prezenţa a patru stari distincte a nucleelor de Fe. În cristalele GaSb dopat cu Fe se formeasă o fracţie cu proprietăţi magnetice bine pronunţate cu compoziţia $FeGa_3$. Această fracţie se formează preponderent la frontiera dintre dislocaţii şi defecte a reţelei cristaline.

Cuvinte-cheie: antimonidul de galiu, izotop-57, Spectrul Mössbauer, investigaţia microscopică

INTRODUCTION

Gallium antimonide (GaSb) is one of binary group's semiconductors with narrow energy bandwidth, low electron effective mass and high mobility. It is a material with crystal lattice and adequate parameters of semiconducting properties suitable for building optoelectronic devices in the range from 0.8 to 4.3 μm. [1-3]. The influence of doping elements belonging to the 3d transitional metals Fe, Ni, Cr, Mn in the binary semiconductors, for instance, the gallium antimonide, on the new physical properties is of high relevance. Among other trends of a special interest is to obtain magnetic materials with polarized electrons in a high spin state, called dilute magnetic semiconductor (DMS) [4]. The most obvious advantage of these materials consists in the possibility to realize magnetic storage information with electronic readout in a single semiconductor device. As was demonstrated in [5] the spin injection may be carried out when electrochemical potentials in the ferro-magnets will be split and the resistance of the ferro-magnet is of comparable magnitude to the contact resistance. Thorough studies of the Fe-Ga system function on the components' ratios and temperature resulted in the publication of the alloys state diagram where are indicating the stable intermetallic compounds and their compositions [6, 7]. The main intermetallic substances obtained are: the cubic **α-Fe_3Ga**, Pm 3 m space group, in the range of 20.6 - 26.3 at.% of Ga and has the solidification temperature, T_c = 588 ^{0}C; the hexagonal β-**Fe_3Ga**, space group $P6_3/mmc$, existing in the limits of 24.3 – 32.0 at.% of Ga and crystallizes between 590 -700 ^{0}C; the monoclinic or tetragonal **Fe_3Ga_4** with composition in at.% Ga between 56.5 – 58.0, the space group C2/m has peritectic formation temperature 906 ± 2 ^{0}C; the β-**Fe_6Ga_5**, R3m space group, containing ~ 45 at. % of Ga, what exists in the narrower range of temperature 770 – 800

^{0}C; the **α-Fe_6Ga_5**, with the same composition, which is characterized by C2/m space group and it is stable at temperature lower 770 ^{0}C; and finally the tetragonal **$FeGa_3$** space group P 4 n2.

According to [8,9] the Fe-Sb phase diagram consists of two phases: stoichiometric $FeSb_2$ and $Fe_{1+x}Sb$. The component $FeSb_2$ is stable in the limits of 45 – 67 at.% of Sb the temperature lowers 738 ^{0}C. The space group of mono-crystal is Pnn2 (FeS_{2-m} type structure)[10]. Each Fe atom is situated in interstitial sites of Sb atoms and is surrounded by six Sb atoms, while Sb atom is surrounded by three nearer iron atoms and one antimony atom. The structure of $FeSb_2$ doesn't change at lower temperatures (4 - 80 ^{0}K), but the quadrupole splitting is changed; FeSb is crystalized in the range of 42 – 48 at.% Sb in $B8_1$ structure type. The antimony atoms form a hexagonal close packed lattice and iron atoms are situated either in octahedral or tetrahedral interstices [11]. The NiAs-type $B8_1$, the phase Fe_3Sb_2 (ε), has a homogeneity range of 40-47 at.% Sb with maximum liquids curve at 1025 ^{0}C [12].

The role of doping atoms in semiconductors could be evidenced via indirect and direct experimental methods. The most ordinary (indirect) methods to investigate the role of doping atoms in a semiconductor host involve measurements of the electrical conductivity, galvanomagnetic effects, photo conductibility, thermo-electrical force etc. These methods, used in the investigation of semiconductor materials, provide the biggest part of information about the role and the state of enclosed atoms in semiconductors. However, the interpretation of data concerning the location of these centres, which can be substitutional, interstitial, and at the limit of the grain or on the vacancy places, requires great caution and finally is based on results obtained by direct methods such as: electronic paramagnetic resonance (EPR), nuclear magnetic resonance (NMR), nuclear quadrupole resonance (NQR), nuclear gamma resonance (Mössbauer spectroscopy, MS), X-ray photoelectron spectroscopy (XPS), perturbed angular correlations (PAC) etc. But these methods are not universal, such as electrical conductivity or Hall Effect measurements, and therefore, they are applicable to a limited number of semiconductors (containing accessible isotopes the case of NMR and Mössbauer, valence and spin state - EPR) or to a restricted set of impurities enclosed atom present in them. It is well- known the role of electronic paramagnetic resonance spectroscopy method to the justified basics theory of the doped centres in semiconductors [13, 14].

During recent years in specific literature it has been accumulated a significant amount of data on doped centers in Fe-Ga, Fe-Sb systems and semiconductors of III-V type obtained by Mössbauer spectroscopy [15-23]. In [24] there was successfully demonstrated the spin injection at room temperature by introducing of Fe_3Si epitaxial layer into GaAs matrix. This result represents an example of ferromagnetic Heusler alloy (Fe_2FeSi) which is a case of favorable spin injection. Considering that the solubility of doping semiconductors of III-V type is effectively small, in order to surpass the difficulties, it was chosen to work far from equilibrium by using epitaxial molecular flow (EMF) at low temperatures. For GaAs system the Curie temperature, T_c, values 60 K [25] and 159 K [26] were obtained. By switching to broadband semiconductors, GaN and ZnO, the values of Tc were significantly increased. Thus, in [27] T_c above 740K was obtained by 3% Mn doping in GaN matrix on Al_2O_3 support. A theoretical study [28] showed that Cr and Mn dopants in cubic 3C-SiC polytype produce a ferromagnetic solid solution for both C and Si position, exhibiting different magnetic moments. Implantation of Fe in SiC did not lead to magnetic phase, but replacement of silicon (Si) by iron (Fe) (at low concentrations) in hexagonal H_6SiC polytype changed the crystal into a ferromagnetic phase. The electrical and optical properties of specified devices are widely affected by the doping material, which is usually realized by diffusion of desired element in semiconducting crystal [29]. The actual study reports on the grown of a p-type gallium antimonide doped with 3 wt.% ^{57}Fe, the related optical and TEM images, and a large set of data obtained using ^{57}Fe

Mossbauer spectroscopy, performed at different temperatures (3-295)K.

MATERIAL AND METHODS

Sample synthesis: Amounts of Ga, m = 0.6545 g; Sb, m= 1.4250 g; and ^{57}Fe, m = 0.0331 g were loaded into optical quartz ampoule with thick-walls (2 to 3) mm and internal diameter ~ 12 mm. The evacuation of the atmosphere alternates with a few washing cycles with argon. At the residual gas pressure of 10-5 mm Hg the ampoule containing sample was sealed and tightly connected to an electromagnetic vibrator (50 Hz) what assured a homogeneous mixture. Both the ampoule and vibrator were placed inside a tube type furnace. A constant temperature of 900 ^{0}C was maintained for 24 hours. Afterwards the electrical supply was switched off and a free cooling of the furnace via its thermal inertia was realized. The obtained product was grinded into a powder and then introduced into the zone melting facility to grow the single crystal via Czochralski method. From the grown single crystal a mass of 0.040 g was separated, grinded into very fine powder and used as a sample (placed in a specific holder) for Mossbauer measurements.

Mössbauer measurements. The Mössbauer spectra were measured via Oxford Instruments Mössbauer-Spectromag 4000 Cryostat from Institute of Inorganic Chemistry, Karlsruhe University. The temperature was varied within 3.0 -300 K. A ^{57}Co source (3.7 GBq) in a rhodium matrix was used. The spectrometer was electrodynamic type with constant acceleration symmetrical waveform. Isomer shifts values are referred to Fe-metal at room temperature. The fits of the experimental data were performed using the wmoss and NORMOSS programs.

X-ray diffraction measurements (XRD) of powder were realized at the Institute of Applied Physics of the Academy of Sciences of Moldova via DPOH-УМ1 equipment. (FeK_α-radiation, Mn filter, $\theta/2\theta$ method.).

Transmission electron microscopy (TEM) images were acquired using a Jeol ARM 200F electron microscope. The ion thinning was performed using a Gatan PIPS model 691 device working at 5kV and 6 degrees incidence. Optical images were obtained using an AXIO-Zeiss- ObserverA1m microscope. For TEM specimen preparation, a slice with a thickness of about 500 microns was cut parallel with the basal plane from the cylindrical GaSb crystal sample, using a diamond wire devices. In a second step, the slice was cut in 9 smaller pieces. Finally, the 0.5mm x 2 mm x 2 mm GaSb piece was mechanically polished on both faces until the thickness of about 30 microns was realized and glued on the 3 mm copper TEM grid. This grid was then ion thinned to obtain a small hole in the middle. The edges of this hole are transparent to the electron beam in the microscope. The TEM specimen was oriented with the microscope axis parallel with the cylindrical axis of the initial cylindrical GaSb sample.

RESULTS AND DISCUSSIONS

Galium antimonide doped with Fe-57 isotope studied in this paper was obtained according with the description in the "experimental part". The Mössbauer spectra (MS) of GaSb-Fe sample (3 at.% of Fe-57) at different temperatures are presented in Fig.1.

At a first glimpse, the most remarkable aspect of the spectra is the existence at rather high temperature of 298 K (RT = room temperature) of three six-line patterns, suggesting the magnetic species for three iron locations. These sextets, also the centrally placed doublet, appeared over the whole temperature range (3-295 K) of Mössbauer measurements. The Mössbauer spectra parameters of investigated sample are presented in the table 1.

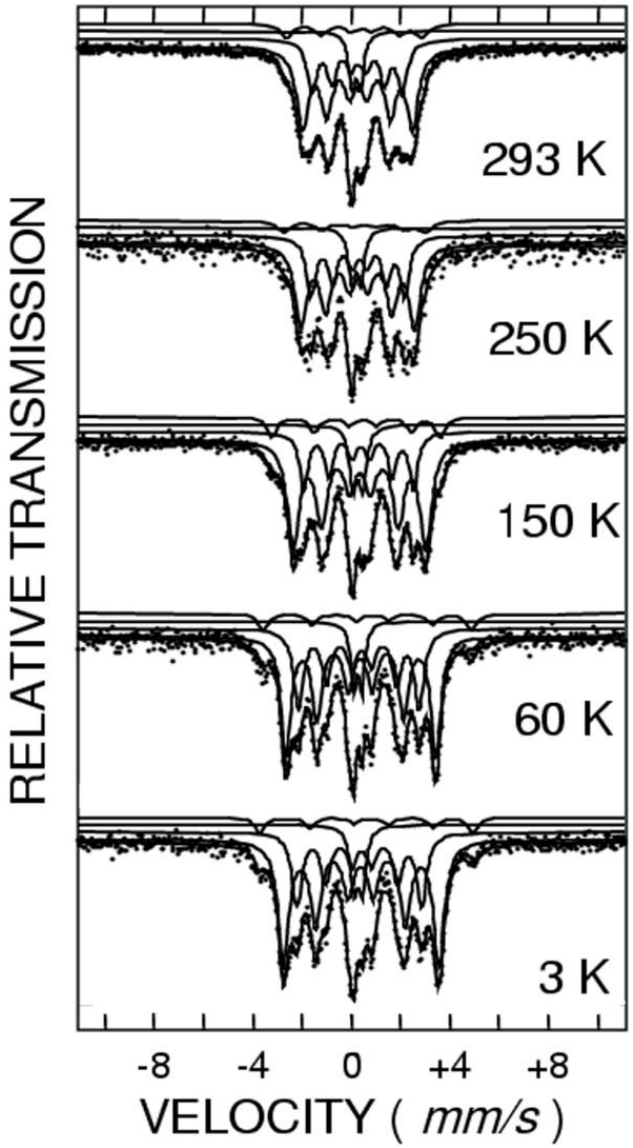

Fig.1. Mössbauer spectra of GaSb-Fe sample (3 at.% of Fe-57) at different temperatures

It is remarkable that the values (last column in the table) of relative area (proportional with amount of Fe ions on every of its location) remain in reasonable limits.

The presence of four different patterns in all exhibited Mössbauer spectra call the attention to a very important experimental feature. An homogeneous distribution of only 3 at.% enriched ^{57}Fe inside the GaSb single crystal lattice (zinc blend cell), substituting either Ga or Sb atoms, normally would provide two doublets, corresponding to both tetrahedral surroundings of Ga and of Sb, showing identical distances to closest neighbours of different type and to second sphere of 12 neighbours of same type as the central ion of the coordination. In such case both the IS and QS will show distinct figures due to peculiar bond of Fe with Ga and, respectively Sb, with higher values for Fe location on Ga sites. Previous attempts of doping with Mn (for example Mn in GaSb [30]) have failed to prove any substitution location. Therefore the presence of Fe in four sites suggest the formation of potentially well crystallized (preparation route) of binary or ternary type compounds. Such phases could exist mainly or only at dislocation or packing defects appearing during single crystal grows. These dislocations are developed preponderantly at the surface of the crystal and evolve inside of the crystal, function of processing temperatures and the stress induced by growing.

Table 1. Mössbauer spectra parameters of GaSb-Fe sample at different temperatures
B_{int} – intern magnetic field around the iron nucleus, error = ± 0.2 T; QS – quadrupole splitting, IS - isomer shift, W - full line width, errors of QS, IS, W = ± 0.02 mm/s; A - relative area, error = ± 1 %; T*- Tesla)

T(K)	Components	B_{int} (T*)	mm/s			A (%)
			QS	IS	W	
3	1	19.5	0.03	0.48	0.56	56
	2	15.7	-0.10	0.48	0.57	30
	3	0.0	0.34	0.39	0.36	8
	4	26.8	-0.22	0.51	0.27	6
60	1	18.8	0.03	0.48	0.47	52
	2	15.2	-0.10	0.47	0.47	34
	3	0.0	0.33	0.38	0.28	7
	4	26.2	-0.21	0.48	0.47	7
150	1	16.7	-0.02	0.45	0.57	59
	2	13.8	-0.07	0.44	0.41	22
	3	0.0	0.39	0.37	0.36	10
	4	21.1	-0.26	0.44	0.39	9
250	1	14.3	-0.03	0.39	0.57	53
	2	11.8	-0.07	0.41	0.46	30
	3	0.0	0.37	0.32	0.32	8
	4	17.9	-0.32	0.40	0.46	9
293	1	13.8	-0.04	0.38	0.58	54
	2	11.4	-0.04	0.37	0.48	29
	3	0.0	0.32	0.31	0.32	8
	4	17.0	-0.23	0.36	0.56	9

Another significant feature is the continuous decrease of the IS with temperature proving the effect of second order Doppler shift [31].

The assignation of the patterns was related to Mössbauer existing data from literature and their analyses in terms of temperature and composition dependence of corroborated parameters.

According to the phase diagram (600 ^{0}C) of ternary FeGaSb system presented in Fig.1 of [12, 32] and phase diagrams of Fe-Ga and Fe-Sb [7, 8], at low concentrations of iron in FeGaSb system may be present the following phases: FeSb, $FeSb_2$, Fe_3Sb_2 (ε), Fe_3Ga, Fe_6Ga_5, Fe_3Ga_4, $FeGa_3$, and epitaxial iron particles at nano-scale [33, 34].

The most facile choice was for the doublet case. Comparing the experimental values of Mössbauer spectra parameters for doublet (component 3) of the sample at RT (IS=0.31 mm/s, QS= 0.32 mm/s) (Table 1) with the literature data for MS doublets of Fe-Sb and Fe-Ga systems [15-17, 34-37] at the same temperature, one can see that they are closest to the diamagnetic $FeGa_3$ [38] (IS=0.28, QS=0.31 mm/s [37]). Checking the structures, the XRD diffractograms (Fig. 2a, 2b) confirm the presence of this compound.

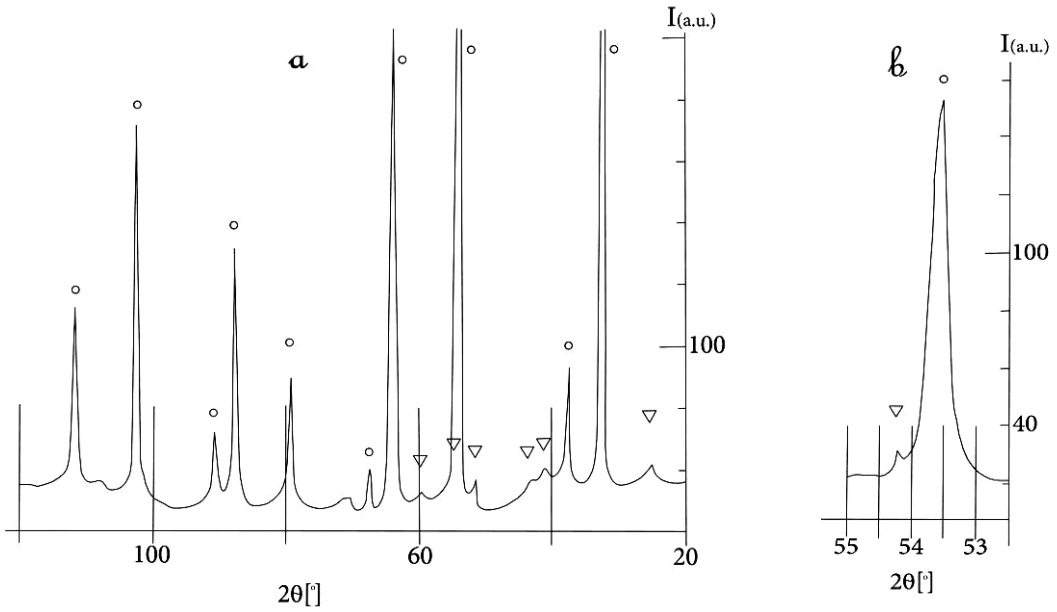

Fig. 2. a) X-Ray powder diffraction spectra of investigated sample GaSb-Fe (3%). o - spectrum's peaks for GaSb. ∇ - peaks for $FeGa_3$ substance. b) Lines separation 220 GaSb (d=2,156 Å) and 212 FeGa3 (d=2,126 Å)

There have been as well other possibilities for a paramagnetic component and among the first of them, it was the presence of $FeSb_2$. However in the actual case it has to be completely excluded because the experimental values of QS (MS) are about 4 times lower (Table 1) than those reported in [15, 17, 18, 39], with values of QS = 1.26-1.29 mm/s and IS = 0.46-0.45 mm/s at RT.

Another alternative was amorphous a-$FeSb_2$ or more close in values of IS and QS the amorphous compound $Fe_{0.5}Sb_{0.5}$ [17] with QS = 0.44; 0.51 mm/s and IS = 0.43, 0.54 mm/s at RT and 4.2K, respectively, but these compounds are definitely out of any consideration, due to the process of growing single crystals. The data of $Fe_{1.3}Sb$ [40, 41] point to a doublet at RT but is showing two sextets, one very pronounced, with B_{int} around 11-12 T and the other one - close to 16-17 T at 5K, therefore are not suitable for our doublet assignation.

As specified above, the studied sample contains three sextet components (labelled 1, 2, 4) with different values of the internal magnetic field, B_{int}, equal to 13.8 T (1), 11.4 T (2) and 17.0 T (4) at 293 K. We note that these values are much lower than that characteristic of α-Fe (B_{int}, 33 T), indicating the formation of systems with the composition $Fe_3(Ga_{1-x}Sb_x)_2$ [19,20], or Fe_3Ga_4 [42], as well Fe_3Ga or $Fe_{1+x}Sb$ [40,41] where x may cover a large range of values. It is worth noticing that from the beginning it was excluded the formation of Fe_3Ga_4 compound [42], where 4 sextets are observed and related IS values are close to zero. The $Fe_{1-x}Ga_x$ alloys were studied in [43], with $0.15 \leq x \leq 0.30$. Those samples, obtained by ball milling, were studied by X-ray powder diffraction, magnetization, electro-conductibility, and Mössbauer spectroscopy methods in the large temperature interval 5 - 770K. The XRD data demonstrated the presence of three crystallographic phases: α (Disorder (bcc)), stable within 15 to 20 at.% Ga; α"(Order (bcc), $FeAl_3$-DO_3), stable within 20-30 at.% Ga; and β (Order (fcc), Cu_3Au=LI_2) stable within 25 -30 at.% Ga. There were determined Curie temperature, T_c, magnetic moment μ (μB) /atom, B_{int}, IS, QS and electro-resistivity. Later, close data were published in [44] for $Fe_{100-x}Ga_x$, where x=15.7, 17.0, 19.0, 22.4, 24.0 obtained by ball milling. In both cases the values of B_{int}, IS and QS differ from our data.

For all magnetic components of here investigated sample the Curie temperatures, TC, are higher than 293K and it is in good agreement with literature data. For example, in the ternary systems $Fe_3(Ga_{1-x}Sb_x)_2$ and $Fe_3Ga_{2-y}As_y$, where $0.1 \leq x \leq 0.75$; $0.21<y$

<1.125, it has been demonstrated by various physical methods the presence of magnetic ordered state with T_C quite high up to 360-374 ^{0}C, and magnetic properties strongly depend on the proportion of Ga and Sb amount surrounding the Fe [19,20, 35,36]. In one attempt to assign the observed 3 magnetically ordered components of the investigated sample we mainly used the results reported for $Fe_3Ga_{2-x}M_x$. According to [20, 35] the systems $Fe_3(Ga_{1-x}Sb_x)_2$ as well $Fe_3(Ga_{1-x}As_x)_2$ have the $B8_2$ hexagonal structure type belonging to P63/mmc space group, which is characteristic for Ni_2In type. In this structure there are two positions of Ni ions: with octahedral (Oh, $NiIn_6$) environment, and one asymmetrical $NiIn_5$ environment. It is obvious that sextets 1st and 2nd should belong to octahedral environment (lower values of QS parameter), but the 4th – one to asymmetrical one. As stated above the most important approach in our analyses was the effect of presence of various elements from pnictide group on B_{int}, IS and eventually QS parameters in Fe_3Ga_2 systems. From this point of view the data from [20, 35] suggest a composition rather poor in Sb and richer in Ga in direct relation with reported data in [20]. Indeed, the Table 9 in [20] revealed that decreasing the Sb content from x=1 to x=0.3 the B_{int} (at RT) augment with 1.5 -1.7 T. Extrapolating, the RT values found for the two octahedral surrounding in our study (Table 1) the observed patterns could stand for a composition with Ga 0.10-0.15 and Sb 1.90 or 1.85. In the study of Smith et all. [20] it was prepared a composition with x=0.10 (T_C data with values around 375K) but any Mössbauer spectrum or parameters were not provided.

The Mössbauer line widths W (Table 1) for the sextets of all three positions are rather large as compared to the line width measured with our source and a standard alpha-Fe absorber (W = 0.25 mm/s). The large line width may be assumed to be an effect of the tiny modified non- equivalent surroundings and to relaxation processes. It should be noted that the mentioned components of the GaSb-Fe system are not formed via substitutions of either Ga or Sb in the GaSb single crystal but are formed at the boundary, hence, their influence on the magnetic, electrical and other properties will be peculiar. Starting to elucidate the above statements, the optical and electron microscopy measurements were envisaged.

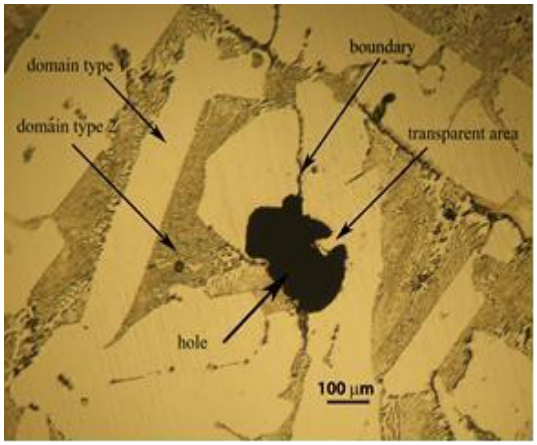

Fig. 3. Optical image (in reflexion) of axis the GaSb-Fe TEM specimen

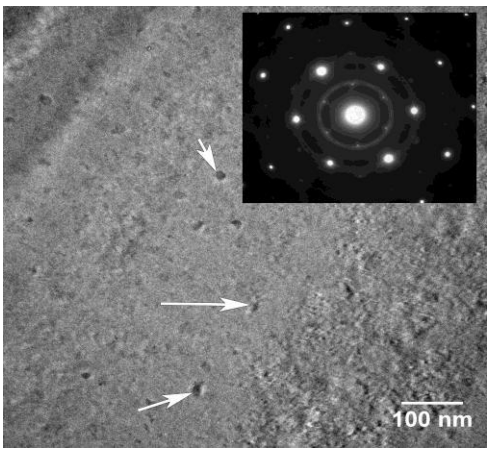

Fig. 4. Domain oriented in <111> zone of the cubic GaSb structure

The reflexion optical image of the "as prepared" TEM specimen is shown in Fig. 3. Two types of crystal domains are observed (transparent and grey) exhibiting large boundaries between them. The optical contrast is due to the ion beam etching for the different crystallographic orientations of the two types of the domains. The areas near the edges of the black hole, situated in the middle of the image in Fig. 3, are transparent areas for the electrons in the microscope. Figure 4 shows a TEM image obtained in such a

transparent areas, representing the GaSb mono crystal structure in <111> orientation, demonstrated by the electron pattern inserted in the figure. The arrows in the Fig.4 show the presence of Ga precipitates on the GaSb TEM specimen surface, after several minutes of observations under the electron beam irradiation, being formed by diffusion of this element from the bulk.

As shown (Fig.5) in the energy dispersive X-ray spectra (EDX), the Fe amount in the crystal bulk areas is less than 0.3 at.%, while in the thick area (Fig. 6) of the specimen, obtained from the location on the boundaries, the Fe is present with about 2.5%. The excess Ga concentration observed in the thin areas of the TEM specimens has two causes. First one, it is the ion thinning process, which changes the sample concentration near the exposed surface, and the second one is the electron irradiation in the microscope, which enhance the Ga diffusion on the TEM specimen surface. After several minutes of observations, nanometric precipitates of Ga appear on the specimen surface, (see Fig. 4). In the thick areas of the TEM specimen, the Ga and Sb concentration resulted from EDX spectra are quite equal, because the amount of the Ga on the surface is less important, comparing to the total amount of the Ga present in the bulk.

As can be observed optically, the boundary regions between the crystal domains are large (about 1 micron) and, as described above, have larger concentration of Fe (2.5 %) comparing to the bulk (less than 0.3 %). This large boundary region, showing also some policrystalline structures, can by explain by the presence of the FeGa3 structure, observed by X ray diffraction.

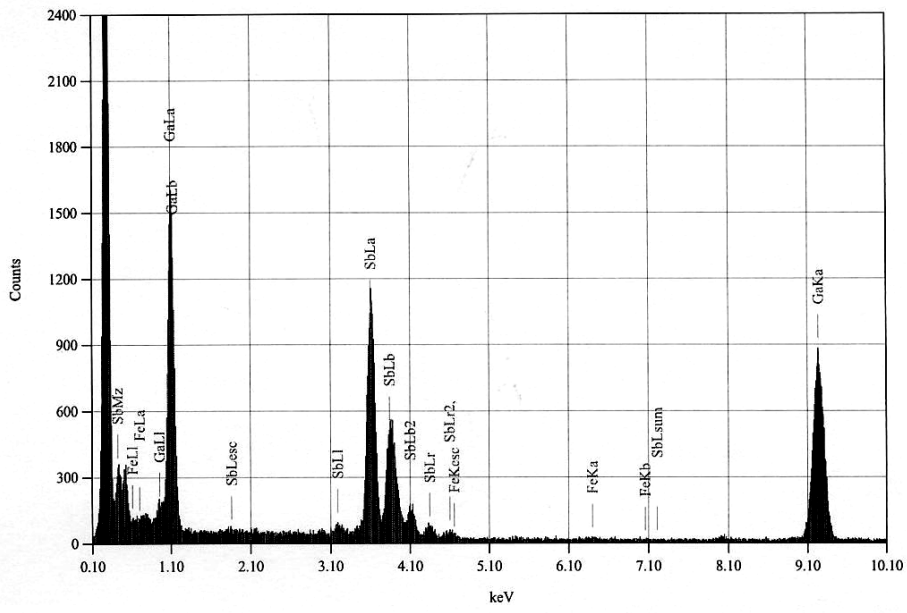

Thin Film Standardless Standard Quantitative Analysis
Fitting Coefficient : 0.5009

Element	(keV)	Mass%	Counts	Error%	Atom%	Compound	Mass%	Cation	K
Fe K	6.398	0.18	128.63	6.73	0.28				0.3986
Ga L	1.098	53.13	12874.93	0.05	66.34				1.1869
Sb L (Ref.)	3.604	46.69	13427.26	0.06	33.38				1.0000
Total		100.00			100.00				

Fig. 5. The EDX spectrum from the thin transparent area of a bulk crystal after TEM observations. The Ga is showing a larger presence on the specimen surface, probably due to the ion thinning process

Due to the complex structure of the boundary region, there was not possible to obtain real transparent areas for TEM in these regions, however the EDX spectra (shown in Fig. 6) could be acquired.

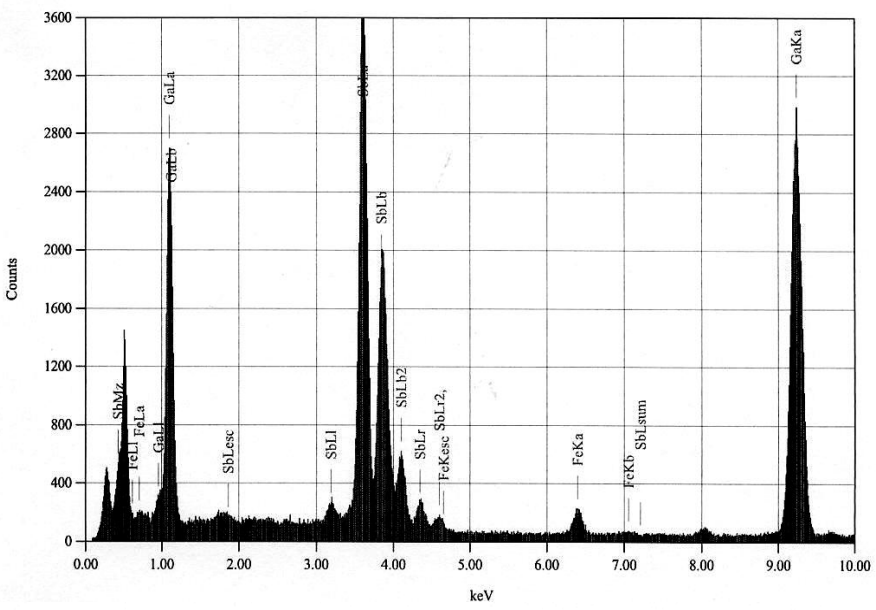

Thin Film Standardless Standard Quantitative Analysis
Fitting Coefficient : 0.2309

Element	(keV)	Mass%	Counts	Error%	Atom%	Compound	Mass%	Cation	K
Fe K	6.398	1.44	2529.94	0.13	2.46				0.3986
Ga L	1.098	34.58	20456.37	0.01	47.36				1.1869
Sb L (Ref.)	3.604	63.98	44918.98	0.01	50.18				1.0000
Total		100.00			100.00				

Fig. 6. EDX spectrum on the thick area of the specimen obtained from an area located on the boundaries between the crystal domains

These results considerably confirm and support the Mössbauer data and the related location of iron containing phases at grain boundaries. Such presence indeed could not substantially influence the physical properties of GaSb single crystal doped with a rather small amount of Fe.

CONCLUSIONS

A single crystal of GaSb doped with 3 at.% Fe, was realized by Czochralski method in order to be investigated using Mössbauer Spectroscopy. The microscopy data, imperiously requested by MS results, revealed the formation of large mono-crystalline domains (GaSb) with optically visible boundaries (large of several microns) and holes between them. The EDX spectrum of the boundary area granted a presence of 2.5 at.% Fe concentration, while in the large domains of the crystal the Fe amount was less than 0.3 at.%.

The first output from Mössbauer data was that Fe does not substitute any of the elements constituting the GaSb single crystal. The Fe is present as binary ($FeGa_3$) and ternary $Fe_3(Ga_{1-x}Sb_x)_2$ phases on the boundary sites between crystallites. Some Mössbauer parameters like isomer shift, line width and fields at nucleus are specifically influenced by the ratio between Ga and Sb in the investigated Fe containing compounds.

REFERENCES

1. Physics of Compounds of Group IV Elements and III-V Compounds. Ed by Madelung O., Landolt-Bornstein New Series, Group 3. Mir. Moscow, 1967.
2. A.G. Milnes, A.Y. Polyakov, Gallium antimonide device related properties, Solid-State Electron. 36, (1993) 803-818.
3. P.S. Dutta, H.L. Bhat, and Vikram Kumar, The physics and technology of galliumantimonide: An emerging optoelectronic material, Journal of Applied Physics. Volume May 81 Issue:9 (1997) 5821 – 5870.
4. H. Ohno, Making, Nonmagnetic Semiconductors Ferromagnetic, Science, 281 no. 5379 (1998) 951-956.
5. G. Schmidt, D. Ferrand, M. Molenkamp, A.T. Filip, and van B.J. Wees, Fundamental obstacle for electrical spin injection from a ferromagnetic metal into a diffusive

Semiconductor, Phys. Rev. B, 62, (2000) R4790-R4793.
6. H. Okamoto, The Fe-Ga (Iron-Gallium) system. ASM International Bull. Alloy Phase Diagrams Vol.11, (1990) No 6, 576-581.
7. H. Okamoto. Fe-Ga (Iron-Gallium)Section III: Suppl. Lit. Review. J. Phase Equilibria and Diff. Vol 25 (2004) No. 1, 100.
8. H. Okamoto: "Fe-Sb (Iron-Antimony)" in Phase Diagrams of Ternary Iron Alloys, ed., ASM International, Materials Park, OH, (1993) pp. 366-370.
9. K.W. Richter. H. Ioser, Reinvestigation of the binary Fe-Sb phase diagram, Journal of Alloys and Compounds, 247 (1997) 247-249.
10. H. Holseth, A. Kjekshus, Copounds with the Marcasite Type Crystal Structure IV. * The Crystal Strucrure of $FeSb_2$. Acta Chimica Scand. 23, No.9, (1969) 3043-3050.
11. M. Sladecek, M. Miglierini, B, Sepiol, H. Ipser, H. Schicketanz and G.Vogl, Diffusion and Mechanism in the Hexagonal B8 of Fe-Sb, Structure of Defect and Diffusion Forum Vols.194-199 (2001) pp.369-374.
12. V. Raghavan. Fe-Ga-Sb (Iron-Gallium-Antimony) JPEDAV (2004) 25:85–86. DOI: 10.1361/10549710417740. 1547-7037/ASM International.
13. E.E.Vogel, and O.Mualin, M.A.de Orue, and J.Rivera-Iratchet. Jahn-Teller effect for Fe^{2+} in III-V semiconductors. Phys.Rev. B, vol.44, number 4, 15 July (1991-II), 1579-1586.
14. Wertz, & J.R. Bolton, Electron spin resonance: Elementary theory and practical applications. New York: McGraw-Hill 1972.
15. Ch.S. Birkel, G. Kieslich, D. Bessas, T. Claudio,| R. Branscheid, U. Kolb, M. Panthofer, R.P. Hermann,| and W. Tremel, Wet Chemical Synthesis and Combined X-ray and Mossbauer Study of the Formation of $FeSb_2$ Nanoparticles, Inorg. Chem. 50 (2011) 11807- 11812.dx.doi.org/10.1021/ic201940r.
16. J.M. Borrego, J.S. Blazqueza, C.F. Conde, A., Conde, S. Rothet. Structural ordering and magnetic properties of arc-melted FeGa alloys, Intermetallics 15 (2007) 193-200.
17. C.L.Chien, Gang Xiao, and K.M.Unruh. Hyperfine interactions and magnetic properties of amorphous Fe-Sb alloys, Physical Review B, Vol.32, numb.9 (1985) 5582-5590.
18. A. Farhan, M. Reissner, A. Leithe-Jasper, and W. Steiner, A high-field Mössbauer investigation on $FeSb_2$, Journal of Physics: Conference Series 217 (2010) 012142 doi:10.1088/1742-6596/217/1/012142.
19. M. Monciardini, L. Pareti, G. Turilli, R. Fomari, A. Paoluzia, F. Albertini, 0. Moze, G. Calestani. Magnetic properties of $Fe_3(Ga_{1-x}Sb_x)_2$, Journal of Magnetism and MagneticMaterials 140-144 (1995) 145-146.
20. N.A. Smith, P.J. Hill, E. Devlin, H. Forsyth, I.R. Harris, B. Cockayne and W.R. MacEwan, Structural and magnetic studies of $B8_2$-type alloys represented by $Fe_3Ga_{2-x}Sb_x$, Journal of Alloys and Compounds, 179 (1992) 111-124.
21. G. Weyer, Defects in semiconductors-results from Mössbauer spectroscopy, Hyperfine Interact (2007) 177, 1–13. DOI 10.1007/s10751-008-9607-y.
22. R. Hu, R.P. Hermann, F. Grandjean, Y. Lee, J.B. Warren, V.F. Mitrović, and C. Petrovic, Weak ferromagnetism in $Fe_{1-x}Co_xSb_2$, PHYSICAL REVIEW B 76 (2007) 224422-1-224422-6, DOI: 10.1103/PhysRevB.76.224422.
23. R.A. Pruitt, W. Marshall., C.M. O'Donnell, Mossbauer Spectroscopy in Group-III Antimonides, Phys. Rev. B 2 nr 7, 1 OCTOBER (1970). 2383-2390.
24. A. Ionescu, C. A.F. Vaz, T. Trypiniotis, G. M.Gurtler, H. Garcia-Miquel, J.A.C. Bland, M. E. Vickers, R.M. Dalgliesh, S. Lanridge, Y. Bugoslavsky, Y. Miyoshi, L.F. Cohen and K. R.A. Ziebeck, Structural, magnetic, electronic, and spin transport properties of epitaxial Fe_3Si/GaAs(001), Phys. Rev. B 71 (2005) 094401-094409.
25. H. Ohno, A. Shen, F. Matsukura, A. Oiwa, A. Endo, S. Katsumoto and Y. Iye, (Ga,Mn)As:A new diluted magnetic semiconductor based GaAs, Appl.Phys.Lett. 69 (1996) 363-365, http://dx.doi.org/10.1063/1.118061 (3 pages).
26. C.T. Foxon, R.P. Campion, K.W. Edmonds, L.Zhao, K.Wang, N.R.S. Farley, C.R. Staddon and B. Gallagher, The growth of high quality GaMnAs films by MBE, Journal of Materials Science: Materialistic Electronics, Vol.15, Num.11 (2005), 727-731,

DOI:10.1023/BJMSE.0000043420.48864.072 004.
27. T. Sasaki, S. Sonoda, Y. Yamamoto, K. Suga, S. Shimizu, K. Kindo and H. Hori, Magnetic and transport characteristics on high Curie temperature ferromagnet of Mn-doped GaN, J. Appl. Phys. 91 (2002). 7911-7913, dx.doi.org/10.1063/1.1451879 (3 pages).
28. V.I. Shaposhnikov and N.A. Sobolev, The electronic structure and magnetic properties of transition metal-doped silicon carbide. J. Phys. Condens. Matter, 16 (2004) 1761-1768.
29. S.Dr. Derek. Chapter 6. Diffusion in Semiconductors, pp.121-135. In the book: Springer Handbook of Electronic and Photonic Materials. Editors: Safa Kasap Prof., Peter Capper Dr. 2007. Doi:10.1088/0953-8984/16/10/008.
30. A. Wolska, K. Lawniczak-Jablonska, M.T. Klepka, A. Barcz, A. Hallen and D. Arvanitis, Study of the Local Environment of Mn Ions Implanted in GaSb, ACTA PHYSICA POLONICA A, Vol. 117 (2010) No. 2. 286-292.
31. R.V. Pound, G.A.Rebka, Gravitational Red-Shift in Nuclear Resonance, Phys. Rev. Letters, 3, (1959) 439-441, DOI:10.1103/PhysRevLett.3.439.
32. S. Deputier, N. Barrier, R. Guerin, and A. Guivarch, Solid state phase equilibria in the Fe- Ga-Sb ternary system at 600 ^{0}C, J. Alloys Compd., 2002, 340, pp. 132-140.
33. D.R.S. Somauajulu, M. Sarkar, N.V. Ptel, K.C. Sebastian and M. Chandra, Mössbauer Study of Magnetic FeSb Dilute SystemHyperfine Interactions 136/137 (2001) 424-431.
34. T.Yu.Kiseleva, E.E. Levin, A.A. Novakova, S.A. Kovaleva, T.F. Grigoreva, A.P. Barinova, N.Z. Lyakhov, Interaction between Iron and liquid Galium in the course ofintensive mechanical activation, Proceed. Tenth Israeli-Russian Bi-National Workshop 2011 "The Optimization of Composition, Structure and Properties of Metals, Oxides, Composites, Nano- and Amorphous Materials", Jerusalem, Israel, June 20-23, 2011, p. 1-9.
35. C. Greaves, E.J. Devlin, N.A. Smith, I.R. Harris, B. Cockayne and W.R. MacEwan. Structural indentification of the new magnetic phases $Fe_3Ga_{2-x}As_x$, Journal of the Less- Common Metals, 157 (1990) 315 – 325.
36. R. Harris, N.A. Smith, E. Devlin, B. Cockayne, W.R. MacEwan, G. Longworth. Structural, magnetic and constitutional studies of a new family of ternary phases based on the compound Fe_3GaAs, Journal of the Less-Common Metals, 146 (1989) 103 – 119.
37. G.L. Whittle, P.E. Clark and R. Cywinski, Vacancies and site occupation in Co-Ga-Fe alloys (Mossbauer study), J. Phys. F: Metal Phys. 10(1980) 2093-2104. Printed in Great Britain.
38. K. Umeo, Y. Hadano, S. Narazu, T. Onimaru, M. A. Avila, and T. Takabatake. F erromagnetic instability in a doped band gap semiconductor $FeGa_3$. PHYSICAL REVIEW B 86, (2012) 144421 -144427.
39. J. Steger and E. Kostiner, Mössbauer effect study of $FeSb_2$, J. Solid State Chem. 5, (1972). 131-135.
40. P.J.Picone, P.E.Clark, Mossbauer measurements on lattice and interstitial iron atoms in $Fe_{1-x}Sb_x$. Journ. Magn. Magnetic Materials, 12 (1979) 233-238.
41. P.J.Picone, P.E.Clark, Magnetic ordering of interstitial iron in Fe_{1-x} Sb_x. Journ. Magn. Magnetic Materials, 25 (1981) 140-146.
42. N.Kawamiya, K.Adachi, Magnetic and Mossbauer Studies of Metamagnetic Fe_3Ga_4, J.Phys.Soc.Jpn. Vol.55, no.2 (1986) 634-640.
43. N.Kawamiya, K.Adachi, Y.Nakamura, Magnetic Properties and Mossbauer Investigations of Fe-Ga Alloys, J.Phys.Soc. Jpn, Vol.33, No.5 (1972) 1318-1327.
44. J.M. Gaudet, T.D. Hatchard, S.P. Farrell, R.A. Dunlap, Properties of Fe-Ga based powders prepared by mechanical alloying, Journal of Magnetism and Magnetic Materials. 320 (2008) 821–829.

Prezentat la redacţie la 30 aprilie 2015